Synthesis and Characterization of Antibody-protected Bimetallic Nanoclusters with Catalytic Properties

Verónica Mora-Sanz[a,b], Laura Saa[a], Nerea Briz[b] and Valeri Pavlov*[a].

[a] Center for Cooperative Research in Biomaterials (CIC biomaGUNE), Basque Research and Technology Alliance (BRTA), Paseo de Miramon 182, 20014, Donostia San Sebastián, Spain
E-mail: vpavlov@cicbiomagune.es

[b] Tecnalia, Basque Research and Technology Alliance (BRTA), Parque Tecnológico de San Sebastián, 2 Paseo Mikeletegi, 20009, Donostia-San Sebastián, Spain

ABSTRACT: In this work a novel and facile method for the synthesis of gold-platinum bimetallic nanoclusters (NCs) embedded in the structure of an IgG (Au/Pt NCs-IgG) is presented. Proteins have been widely used as scaffolds for the synthesis of atomic clusters. The harsh conditions usually required during the synthesis imply the denaturation of different proteins and the loss of their biological activity. We propose a strategy for the synthesis of NCs employing IgG as a scaffold performed using physiological conditions in order to maintain unalterable the IgG structure allowing the resulting material bind to Protein G and the antigen. NCs composed of two different types of atoms exhibit higher catalytic activity than monometallic nanoclusters (NC), due to the synergistic effect of two diverse atoms. This peroxidase-like activity and the maintained affinity for its antigen make Au/Pt NCs-IgG a suitable material for its use as a detection antibody in a direct sandwich Enzyme-Linked Immuno Sorbent Assay (ELISA). Use of Au/Pt NCs-IgG as an alternative to IgG tethered to horseradish peroxidase in ELISA boosts the limit of detection (LOD) by 56 times.

INTRODUCTION. Immunoassays are analytical techniques in which the selectivity and sensitivity are provided by the specific interaction between an antibody and its target analyte [1]. Enzyme-linked immunosorbent assay (ELISA) taking advantage of enzymes attached to the antibody like horseradish peroxidase (HRP) or alkaline phosphatase (ALP) for signal amplification is the most frequently employed method in clinical diagnostics [2, 3, 4, 5]. Natural enzymes as markers have several disadvantages, for instance, high susceptibility to environmental variations, easy denaturation and digestion, costly and time-consuming preparation and purification [6]. Enzymes and antibodies are incubated with crosslinking reagents and then the conjugate is purified. Some of the most commonly used crosslinking reagents are glutaraldehyde [7], periodate [8] and maleimide [9]. Different reactivities of enzymes and antibodies with respect to crosslinkers result in the formation of heteropolymers (IgG-enzyme) and homopolymers (IgG-IgG and enzyme-enzyme) by random coupling. Polymers in which antibodies are not completely reactive may not be eliminated by conventional purification processes and cause high background signals and low precision due to nonspecific absorption of heteropolymers, while homopolymers are of no use at all for detection of analytes. These methods are not suitable for ultrasensitive enzyme immunoassays[10]. Antibodies and enzymes can be indirectly and non-covalently crosslinked via the strong affinity between biotin and avidin [11]. A feature of this method is signal amplification achieved by introduction of many biotin residues into antibody molecules and subsequent binding of avidin linked to enzyme molecules. However, nonspecific binding is also amplified. Therefore, new labels for biomolecules that give unequivocal signal and promote conservation of sufficient biological activity for use in bioassays are required. Interesting nanomaterials mimicking enzymes, such as, inorganic materials showing catalysis [12,13,14,15], carbon nanomaterials [16,17], noble-metal nanoparticles [18,19,20], and metallic nanoclusters (NCs)[21] have been reported.

NCs with sizes between 0.2 to 3 nm [22,23] made of a few to roughly several hundred metal atoms. NCs are characterized by a size comparable with the dimension of the Fermi wavelength of electrons and they exhibit molecule-like properties [24,25]. Several biopolymers like bovine serum albumin (BSA) [25,26,27], lysozyme [28,29], glucose oxidase (GOx) [30], HRP [31], glutathione [32] or DNA [33] have been used to make stable clusters of atoms. The synthesis of NCs stabilized with proteins usually is carried out under extreme conditions in terms of pH or tem perature, which cause the denaturation of the proteins. The antibody structure includes four polypeptidic chains linked through –S-S- bridges. Sulphur atoms abounding in the central hinge region of IgG macromolecules make them suitable templates for the synthesis of NCs. We present a method to

produce catalytic bimetallic NCs composed of gold and platinum atoms using antibodies as a scaffold. The antibody-antigen system consisting of BSA and corresponding anti-BSA IgG was selected as a model. The peroxidase-like activity of NCs can be used for signal amplification in a direct sandwich ELISA.

EXPERIMENTAL SECTION

Materials. Chloroauric acid ($HAuCl_4$), potassium tetracholoroplatinate (K_2PtCl_4), sodium borohydride ($NaBH_4$), Bovine Serum Albumin (BSA), polyclonal anti-BSA IgG (developed in rabbit), 3,3',5,5'-Tetramethylbenzidine (TMB), TMB liquid substrate system for ELISA, Amplex Red, , phosphate buffered saline (pH 7.4) (PBS), sodium phosphate monobasic (NaH_2PO_4), TWEEN-20 and other chemicals were purchased from Sigma (www.sigmaaldrich.com, St. Louis, MO, USA). Hydrogen peroxide (H_2O_2) was supplied by Panreac (Barcelona, Spain). Polyclonal anti-BSA IgG (developed in chicken) was supplied by Abyntek (www.abyntek.com, Derio, España). Polyclonal Rabbit Anti-Human Prostate-Specific antigen (PSA) IgG was supplied by Dako (Agilent, www.agilent.com, CA, USA). PSA was commercially available from Lee BioSolutions (www.leebio.com, MO, USA). HRP conjugation kit HRP Lightning-Link® (ab102890) was obtained from Abcam (www.abcam.com, Cambridge, UK). One µm diameter polyvinyl chloride microbeads decorated with Protein G (beadBALL-Protein G) were purchased from Chemicell GmbH (www.chemicell.com, Berlin, Germany).

Characterization.UV-visible measurements were performed on a Varioskan Flash microplate reader (Thermo Scientific) controlled by SkanIt Software 2.4.3. Transmission electron microscope (TEM) images were obtained in JEM-2100F [Model EM-20014, UHR, 200 kV] (JEOL, Japan) equipped with a digital camera of type F-216 (TVIPS, Germany). Scanning transmission electron microscopy (STEM) samples were prepared by desiccating a small droplet of the freshly prepared solution on the hydrophilized surface of an ultrathin carbon film coated Cu-grid. Energy-dispersive X-ray (EDX) elemental maps were acquired using a probe-corrected Titan electron microscope (Thermo Fisher) equipped with a Super-X detector, operated at 300 kV. Elemental maps were obtained over the course of 40 min at 150 pA electron beam current. Data analysis was performed using Bruker Esprit software. X-ray photoelectron spectroscopy (XPS) measurements were performed in a SPECS Sage HR 100 spectrometer with a non-monochromatic X-ray source (Magnesium Kα line of 1253.6 eV energy and 252 W), which was placed in perpendicular position to the analyzer axis and calibrated using the $3d_{5/2}$ line of Ag with a full width at half maximum (FWHM) of 1.1 eV. The selected resolution for the spectra was 0.15 eV/step and 15 eV of Pass Energy. All experiments were completed in an ultra-high vacuum (UHV) chamber at a pressure around 8.10^{-8} mbar. An electron flood gun was used to neutralize for charging. Samples were deposited on carbon adhesive tabs and dried in a Desiccator Cabinet (Scienceware®) for 48 hours. Circular dichroism (CD) spectra were recorded in a JASCO J-815CD Spectrometer using a 1 mm path length quartz cuvette, with a band-width of 1 nm, at increments of 1 nm and 10 s average time. Matrix Assisted Laser Desorption/Ionization time-of-flight (MALDI-TOF) spectra were recorded in a MALDI/TOF-TOF MS UltrafleXtreme III (Bruker) controlled by Flex Control 3.3 software. For the MALDI-TOF sample preparation, the thin layer method and a mixture of two matrixes were used[34]. For the thin layer preparation, a drop of saturated solution of α-Cyano-4-hydroxycinnamic acid (α-CHCA) in acetone was deposited on the MALDI target The matrix solution was prepared by mixing 1:1 ratio (vol/vol) of 20 mg/mL of α-CHCA in ACN (acetonitrile) and 5% formic acid (70:30, vol/vol) and a 20 mg/mL of DHB (2,5-dihydroxybenzoic acid) in ACN and 0.1% TFA (trifluoroacetic acid) (70:30, vol/vol). Finally, the sample (0.5 µL) was mixed with of matrix solution (0.5 µL) and deposited on the thin layer previously deposited on the MALDI target.

Synthesis of Au/Pt NCs-IgG. A solution of polyclonal anti-BSA antibody from rabbit (100 µL, 1 mg/mL) in phosphate buffer (10 mM, pH 7.0) was mixed with $HAuCl_4$ (50 µL, 250µM) and K_2PtCl_4 (120 µL, 500 µM) and incubated for 30 minutes in the dark. In order to initiate the reduction of the metal ions, a freshly prepared solution of $NaBH_4$ (30 µL, 10 mM) was added under vigorous stirring and the colour of the mixture changed from colourless to pale brown. The solution was incubated for three hours at room temperature (RT) and filtrated to separate the free ions from the atoms forming NCs, using Amicon filters of molecular weight cut-off of 30 kDa.,for 15 min, at 10000 x g).

Labeling of Anti-BSA IgG with HRP*:* The conjugation of Anti-BSA IgG (from rabbit) with HRP was performed using a kit purchased from Abcam (HRP Conjugation Kit - Lightning-Link® (ab102890)). First, the modifier reagent (10 µL) was added to a solution of polyclonal Anti-BSA IgG from rabbit (100 µL, 4 mg/mL). Then, this mixture was added to the lyophilized HRP, resuspended and incubated for 3 hours. Afterwards, the quencher reagent (10 µL) was added. The resulting HRP labelled IgG did not require further purification and was used after 30 minutes.

Catalytic Activity Evaluation of Au/Pt NCs-IgG: The peroxidase-like activity of Au/Pt NCs-IgG was analysed by calculating steady-state kinetic parameters. The assays were carried out at room temperature in 96-well Nunc MaxiSorp clear microplates. The peroxidase activity of Au/Pt NCs-IgG was measured using the chromogenic substrate TMB. The reaction mixture (final volume 100 µL) was composed of Au/Pt NCs-IgG in citrate buffer (10 mM, pH=4.0) containing varying concentrations of TMB at a fixed concentration of H_2O_2 or *vice versa*. The colour change of the solution, due to oxidation of substrateTMB, from colourless to blue was registered along the time at an absorption wavelength of 655 nm. The Michaelis-Menten constant (Km), which is an indicator of enzyme affinity for its substrate was obtained by using Lineweaver-Burk plot:

$$\frac{1}{v} = \frac{K_m}{V_{max}} \cdot \frac{1}{[S]} + \frac{1}{V_{max}}$$

Where v is the initial velocity, [S] is the concentration of the substrate, and V_{max} is the maximal reaction velocity.

Modification of Protein G decorated Polyvinyl Chloride Microbeads with Au/Pt NCs-IgG: Commercially available protein G-decorated microbeads (200 µL, 10 mg mL^{-1}) were centrifuged (500 g, 1 min) and the supernatant was discarded. Beads were washed three times with PBS (200 µL, pH 7.4)

and resuspended in PBS (200 µL). 100 µL of the Protein G-beads were mixed with 100 µL of Au/Pt NCs-IgG or Au/Pt NCs-BSA in separated tubes. The concentration of added proteins was 0.33 mg/mL in both cases. Samples were allowed to react for 15 minutes at RT and centrifuged, to separate non-bound molecules from the proteins bound to microbeads. After, the beads were washed three times with PBS/0.05% (v/v) Tween (PBST) and resuspended in PBS (100 µL).

Direct immunoassay for detection of BSA based on the catalytic activity of Au/Pt NCs-IgG: The experiments were carried out in 96-well Nunc MaxiSorp clear microplates. First, different BSA concentrations (100 µL) in PBS were added into the wells and incubated overnight at 4 °C. Then, a blocking solution of casein (100 µL, 20.5 mg/mL) was added and incubated for1 h at RT. Next, Au/Pt NCs-IgG (100 µL, 33 µg/mL) was added and incubated (1h, RT). After each step the wells were washed three times with PBST (100 µL). Finally, a mixture (100 µL) of TMB (200 µM) and H_2O_2 (250 mM) was added to the wells in order to measure the catalytic activity of Au/Pt NCs-IgG. The increase in the absorbance at 655 nm was monitored.

Fab and F(ab')2 fragments generation: Fab and $F(ab')_2$ fragments were prepared using Pierce™ Fab Micro Preparation Kit and Pierce™ $F(ab')_2$ Micro Preparation Kit (Thermo Fisher Scientific), respectively, from intact rabbit anti BSA IgG antibodies. For generation of Fab fragments, immobilized papain digests IgG antibodies, and Fab fragments are purified using Protein A agarose. For production of $F(ab')_2$, immobilized pepsin protease is employed. Fab and $F(ab´)_2$ fragments were used for the synthesis of Au/Pt NCs, following the same protocol described in Experimental Section for the intact Anti-BSA IgG antibody. Afterwards, the resulting solutions were employed for detection of BSA in a direct ELISA assay, as described in Experimental section.

Direct sandwich ELISA for detection of BSA based on the catalytic activity of Au/Pt NCs Anti-BSA IgG: The immunoassays were carried out in Nunc MaxiSorp 96-well clear microplates. Capture antibody Anti-BSA developed in chicken (100 µL, 10 µg/mL) was immobilised on the surface of a microplate (2 hours, 37 °C). Next, the surface was blocked with casein (100 µL, 20.5 mg/mL) and incubated overnight at 4 °C. Different concentrations of BSA were added in different wells and incubated (1 h, RT). After, Au/Pt NCs-anti-BSA IgG (from rabbit) (100 µL, 33 µg/mL) was added and incubated (1 h, RT). After each step the wells were washed three times with PBST (100 µL). Finally, a solution (100 µL) of TMB (200 µM) and H_2O_2 (250 mM) was added to the microplate wells and the change in the absorbance at 655 nm was monitored on the standard plate reader during 4 min.

Direct sandwich ELISA for detection of BSA based on the catalytic activity of HRP labelled Anti-BSA IgG. In order to compare the presented system with the conventional assay using HRP, direct sandwich ELISA for BSA based on the catalytic activity of Anti-BSA IgG/HRP (from rabbit) was performed. For that, the same procedure was followed as described above but instead of Au/Pt NCs-anti-BSA IgG (from rabbit) as detection antibody, we employed the same antibody anti-BSA IgG (from rabbit) labelled with HRP. For the peroxidase activity detection, commercially available TMB liquid substrate system for ELISA was employed.

RESULTS AND DISCUSSION

Synthesis and characterization of Au/Pt NCs-IgG. Bimetallic clusters of atoms composed of gold and platinum using Anti-BSA IgG as scaffold were synthesized according to the procedure reported in Experimental section. In Fig. 1 the synthetic route to IgGs containing inside Au/Pt NCs is represented. Different concentrations of the reagents were tested before choosing the optimal experimental conditions (Table S1). The optimisation was carried out based on the performance of the catalytic Au/Pt NCs-IgG in a direct ELISA. In Fig. S1 the rate of 3,3′,5,5′-Tetramethylbenzidine (TMB) oxidation to the resulting diimine is represented vs. various synthetic conditions. The fastest oxidation rate of this chromogenic compound was obtained at a final concentration of 0.33 mg/mL for Anti-BSA IgG, 41.5 µM for $HAuCl_4$, 200 µM for K_2PtCl_4 and 1 mM for $NaBH_4$. Further experiments were carried out using these conditions. Scanning transmission electron microscopy (STEM) was used to determine the morphology and the size of Au/Pt NCs-IgG. In Fig. 2A the spherical shape of the NCs is revealed. Using the statistics analysis of 100 individual NCs the representative size was determined to be 1.97 ± 0.71 nm (Fig. 2B).

XPS was used to analyse the valence status of metallic nanoclusters. Fig. 2C shows the Pt4f spectra of Au/Pt NCs-IgG. This spectrum is composed of two energy bands. On the one hand the Pt4f7/2 energy band is evident and on the other hand Pt4f5/2 bands of energy at 71.1 eV and 74.2 eV respectively can be seen. Such distribution of bands is characteristic of Pt in metallic state [35]. The Pt4f7/2 spectrum was fitted tot-wo curves, one asymetric Lorentzian curve in the case of Pt(0) (71 eV) and a symmetric Gaussian-Lorentzian curve for Pt(II) (72,4 eV). These peaks are usually found at 71 eV and 72.4 eV[36]. In the Au 4f region the spectra presents characteristic doublet with the 4f7/2 and 4f5/2 energy bands separated by 3.67 eV. The Au4f7/2 can be deconvoluted to two curves, one for Au(0) (83.1 eV) and another for Au(I) (84.8 eV). These peaks usually appear at binding energies of 84 eV and 85 eV respectively [37].The difference between the widespread values and the NCs values suggest a strong interaction between Au and Pt atoms with the consequent formation of Au-Pt alloys as will be demonstrated below. This effect has been observed in other bimetallic NCs [6].

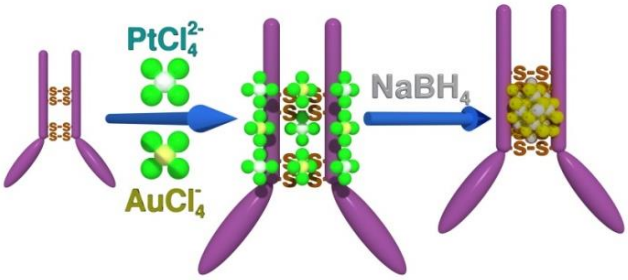

Figure 1. Schematic representation of the synthesis of bimetallic Au/ Pt NCs protected by antibodies.

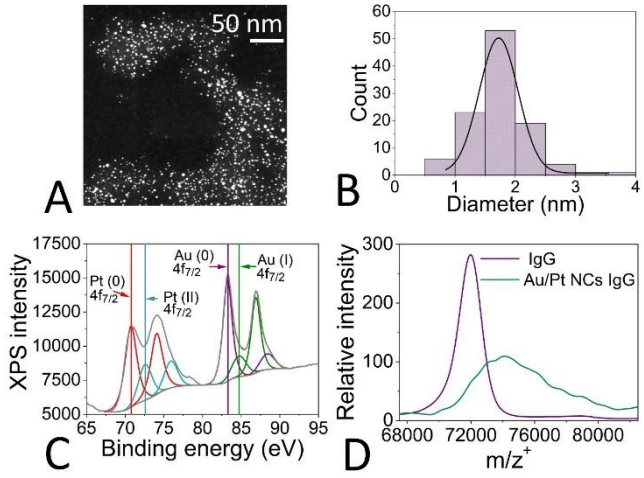

Figure 2. STEM image (a), size distribution (b) and spectra of XPS (c) of Au/Pt NCs synthesized inside of IgG. MALDI-TOF mass spectra of pristine Anti-BSA IgG (purple) and anti BSA IgG carrying Au/Pt NCs- (green), (m/z+, z=2) (d).

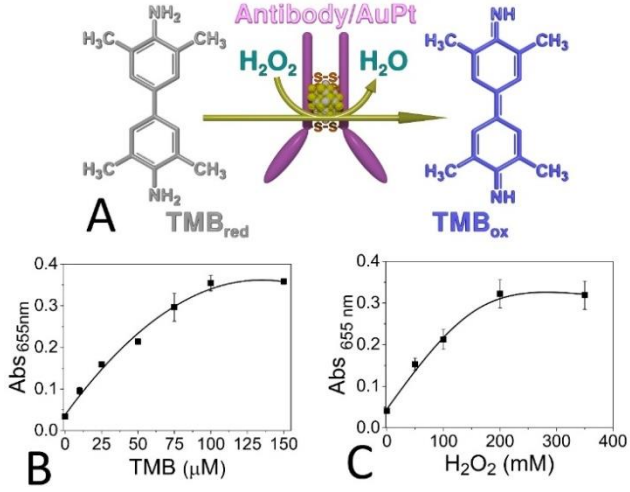

Figure 3. (a) Scheme of TMB oxidation in the presence of H_2O_2 catalyzed by Au/Pt NCs-IgG. Intensity of absorbance peak (655 nm) at different (b) TMB and (c) H_2O_2 concentrations.

MALDI-TOF analysis was performed for verification of binding of the metallic NCs to the IgG structure. The intensity vs. m/z (mass-to-charge ratio) plots (m/z+, z=2) for the pristine antibody and Au/Pt NCs-IgG is shown in Fig. 2D. A shift of the peak corresponding to the NC-containing sample towards greater masses can be observed. From the analysis of the spectrum one can conclude that metallic NCs are bound to IgG macromolecules having affinity to BSA. Despite the appearance of the mass peak shift in the spectrum, the accurate evaluation of mass of bimetallic NCs could not be performed due to several issues such as, broad spectral peaks and contradictions between STEM and MALDI-TOF results. The mass peaks of pristine IgG and modified IgG are broad due to the use of a polyclonal antibody that has a polydispersed mass and the polydispersity of metallic cores observed in STEM images (Fig. 2b). STEM images show larger size of NCs compared to that obtained in MALDI-TOF because STEM frequently causes aggregation of NC on the carbon grids used as substrates [28,38]. Also, the larger weight of IgG carrying NCs, decreases their propensity to ionization.. Hence, larger NCs are not detected by MALDI-TOF. [39,40]

Catalytic activity of Au/Pt NCs-IgG. Au/Pt IgGs modified with Au/Pt nanoclusters have peroxidase-like activity and can mimic the behavior of the commonly used enzyme HRP. Both, NCs and HRP are able to oxidize the chromogenic substrate TMB in the presence of H_2O_2 (Fig. 3A). This substrate changes its colour from colourless in its reduced state to blue in its oxidized form. TMB and H_2O_2 concentrations affect the rate of the redox reaction catalyzed by Au/Pt NCs-IgG. To measure the dependence of the initial reaction rate on concentration of both substrates, the concentration of one of the substrates was fixed while the concentration of other one was changed. In both cases the Au/Pt NCs- IgG concentration was kept constant at 33 µg/mL (referred to as Anti-BSA IgG concentration).

In Fig. 3B and Fig. 3C it is shown how the reaction rate of TMB oxidation increases with the rise of substrate concentration following a Michaelis-Menten like kinetics. The Michaelis-Menten constant (K_m) was obtained with the Lineweaver-Burk equation. The value of K_m is the measure of the affinity of enzymes for their substrates. The stronger is the affinity, the lower is the K_m [41,42]. In Table S2 the K_m values for Au/Pt NCs-IgG and HRP[6] are compared. The $K_m$value of Au/Pt NCs IgG is more than 8.5 times lower than that of HRP towards TMB, which indicates that Au/Pt NCs-IgG has a higher affinity than HRP to TMB as a substrate. While the value of K_m for Au/Pt NCs IgG is significantly higher than that for HRP to H_2O_2, indicating Au/Pt NCs IgG has a lower affinity for H_2O_2 than HRP. This phenomena has been also observed in case of nanozymes.[43, 44] In order to evaluate stability of Au/Pt NCs IgG a fresh solution of anti-BSA antibody was prepared using the optimized synthesis procedure. Then, the peroxidase like activity of the resulting modified antibody was measured under the same experimental conditions during several days after the synthesis. During this period of time the solution of Au/Pt NCs IgG was kept at 4 °C in the fridge. According to this stability study (Figure S2, in Supporting Information) half-life of the active bimetallic clusters was around 10 days. Such stability of Au/Pt NCs-IgG was sufficient to validate this nanomaterial in immunoassays, for the reason that the employment of modified antibodies in bio-assays is usually limited to several hours. The shelf life of the produced Au/Pt NCs-IgG was studied in the absence of any stabilizers because optimization of storage conditions was not among the priorities of this work. Potentially the shelf life can be extended by using more appropriate storage conditions such as addition of preservatives, lyophilisation of Au/Pt NCs-IgG and oxygen elimination. Extension of the shelf life of Au/Pt NCs-IgG under optimized storage conditions can become a main goal of a future investigation.

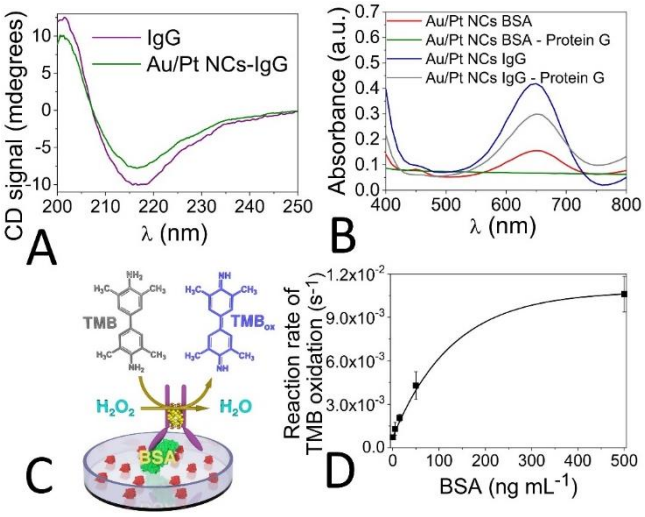

Figure 4. (a) Far-UV CD spectra of IgG and Au/Pt NCs-IgG. (b) Catalytic properties of Au/Pt NCs-IgG and Au/Pt NCs-BSA with TMB in the presence of H_2O_2 incubated with microbeads decorated by Protein G and free in solution. (c) Schematic representation of a direct immunoassay for BSA usingAu/Pt NCs-IgG as detection antibody. (d) Calibration curve of BSA obtained in a direct ELISA assay based on Au/Pt NCs-IgG using λ=655 nm.

Antibody structure stability after the synthesis of NCs. Most of the methods described in literature about the synthesis of metallic NCs using proteins as scaffold uses harsh conditions that result in the negative alteration of their biological functions [25]. The final goal of this study is to validate application of the catalytic properties of NCs, embedded in an antibody structure, to an immunoassay, therefore ideally the structure of the antibody and its affinity for a target analyte should not change during the synthesis of the NCs. Different experiments were performed to test if the antibody structure is changed in the course of NC synthesis. CD spectroscopy was used to characterize the secondary structure and conformation of proteins[45]. Far-UV CD spectra (180-250) reveal the secondary predominant structure for IgG composed f antiparallel β-sheet and random coil conformations [46]. The presence of β-sheets can be detected by the presence of a broad minimum at 218 nm in the far-UV CD spectra [45]. After the synthesis of metallic NCs using an antibody as a scaffold its secondary structure could be damaged or completely disappear. However, in the CD spectra of the pristine antibody and Au/Pt NCs-IgG shown in Fig. 4A, no significant differences between both plots are evident, so it can be concluded that the metallization of Au/Pt NCs inside of IgG does not cause any detectable change in the IgG conformation. In order to check out if the fragment crystallizable (Fc) region of the antibody, which interacts with Fc receptors of some proteins[47] , still maintains affinity to Protein G after the introduction of NCs into the antibody structure those modified IgGs were captured on the surface of polyvinyl chloride microbeads bearing protein G . The microbeads were mixed with Au/Pt NCs-IgG as described in the experimental section. As a control Au/Pt NCs synthesized using BSA as scaffold were used. It is known that BSA does not bind to Protein G so no immobilization of NCs on microbeads of this kind should be detected. The catalytic properties of Au/ Pt NCs-IgG and Au/Pt NCs-BSA were used to verify the binding to the microbeads. After the incubation of microbeads with both types of NCs, the solutions were centrifuged, and after removal of the supernatant microbeads were washed three times in a centrifuge. Then, a solution containing TMB and H_2O_2 was mixed with the pellets and the rate of TMB oxidation was determined by UV-Vis spectroscopy. The catalytic activity of TBM oxidation shown by the pellets was compared with that of free Au/Pt NCs-IgG and Au/Pt NCs-BSA in solution (Fig. 4B). Free Au/Pt NCs-IgG exhibit catalytic activity in a bulk solution. Microbeads tethered to Au/Pt NCs-IgG via Protein G demonstrated catalytic activity too. Catalytic oxidation of TMB was observed in the presence of free Au/Pt NCs-BSA. However, microbeads decorated with Protein G do not show catalytic activity after incubation with Au/Pt NCs-BSA. This observation demonstrates that the Fc of antibodies was not significantly changed during the metallization of Au/Pt NCs inside of IgG, therefore the resulting modified IgG stall retains affinity to Protein G. In addition, this binding to Protein G –modified microbeads is very specific only for Au/Pt NCs IgG.

The affinity of the Au/Pt NCs-IgG for its target analyte was studied with a direct immunoassay. In Fig. 4C the scheme of the direct immunoassay based on the catalytic properties of Au/Pt NCs-IgG is shown. Different BSA concentrations (0 to 500 ng/mL) were adsorbed on a microplate. The calibration curve (Fig. 4D) demonstrates the dependence of the initial oxidation rate of TMB, which was registered during the first 4 minutes, in the increasing concentrations of TMB. According to the observed experimental data IgG carrying bimetallic nanoclusters still retains affinity to its target molecules and can be used as a detection antibody in a direct sandwich ELISA.

Evaluation of the bimetallic composition of the Au/Pt NCs cores and its position in the antibody structure. In order to elucidate the region of the antibodies involved in the stabilization of Au/Pt NCs, different antibody fragments were produced and used as scaffolds for the synthesis of NCs. A representative SDS-PAGE gel of the obtained fragments is depicted in Fig. S3. Afterwards, the performance of the resulting antibody fragments modified with Au/Pt NCs in a direct ELISA assay for the detection of BSA was evaluated. Antigen binding fragment (Fab) is a region on an antibody that binds to antigens, and F(ab')2 fragments have two antigen-binding Fab parts bound by disulfide bonds. In the ELISA assay, in the case of using Au/PtNCs Fab fragments for stabilization of NCs, no peroxidase activity was detected (Fig. 5A), whereas this activity was detected in the sample corresponding to the incubation with Au/Pt F(ab')2 and the intact antibody. These results suggest that the hinge region of the antibodies, rich in disulphide bonds, could play an important role in the Au/Pt NCs stabilization. Only F(ab')2 fragments form composites with peroxidase like activity showing affinity to BSA and Fab fragments are not able to yield such composites. This means that bimetallic NCs are not metallized within Fab fragments in close vicinity to antigen binding sites. Given the medium diameter of bimetallic clusters of 1.8 nm and overall

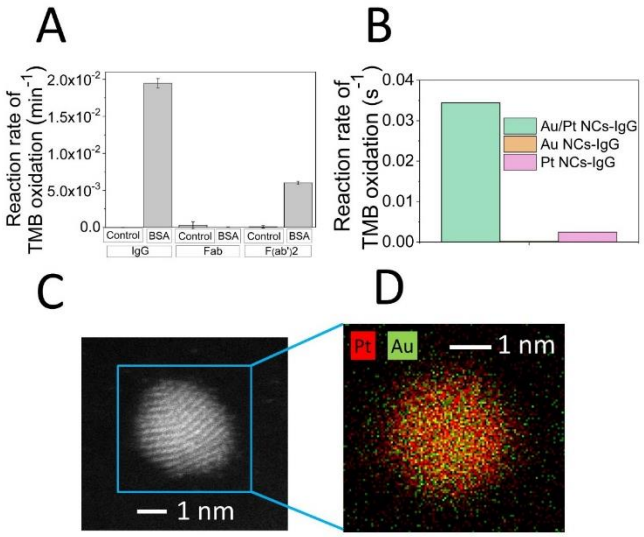

Figure 5. (a) Reaction rate of TMB oxidation in the direct ELISA performed with Au/Pt NCs IgG, Au/Pt NCs Fab and Au/Pt NCs F(ab')2 fragments in the absence (control) or presence of 200 ng/ml BSA. (b) Reaction rate of TMB oxidation of Au/Pt NCs-IgG, Au NCs-IgG and Pt NCs-IgG. (c) TEM image of a single Au/Pt NCs-IgG. (d) EDX mapping of the single Au/Pt NCs-IgG.

dimensions of IgG (14.5 nm × 8.5 nm × 4.0 nm), with antigen bind ing sites separated by 13.7 nm[48, 49] it can be concluded that, most probably, bimetallic clusters are located exactly at the hinge region of the antibodies, sufficiently far away from binding sites. Therefore, in majority of produced Au/Pt NCs IgG metallization does not sequester active sites on antibodies due to small size of NCs and their well defined position at the center of IgG macromolecules.

In order to confirm that the catalytic activity of the Au/Pt NCs-IgG is related with the presence of both metals the synthesis of the NCs was carried out three times. One of the syntheses was carried out without the addition of K_2PtCl_4, therefore monometallic NCs composed by gold were synthesized (Au NCs-IgG). The second synthesis was performed without the addition of $HAuCl_4$ in order to prepare monometallic NCs composed of platinum (Pt NCs-IgG). The third synthesis of Au/Pt NCs-IgG was carried out as usual (with both metal precursors). A direct sandwich ELISA was used to compare applicability to immunoassays of the next three modified IgGs: Au NCs-IgG, Pt NCs-IgG and Au/Pt NCs IgG.

The reaction rate for each NCs is shown in Fig. 5B. The maximum reaction rate of TMB oxidation was found for Au/Pt NCs-IgG. Very low catalytic activity was achieved with Pt NCs-IgG in comparison with that shown by Au/Pt NCs-IgG and no catalytic activity was observed with Au NCs-IgG. These results suggest that the presence of both metal precursors is necessary during the synthesis to achieve the formation of catalytic NCs. The synergistic effect between Au and Pt atoms was observed in other Au/Pt bimetallic NCs [6] .EDX mapping of a single Au/Pt NC IgG (Fig. 5C) was used to further confirm the bimetallic composition of NCs. The red dots belong to Pt atoms and the green ones to Au atoms (Fig. 5D) with an atomic percentage of 91 and 9 % respectively. The results of this experiment confirm that effectively Au/Pt NCs-IgG have a bimetallic composition.

Performance of sandwich ELISA using Au/Pt NCs-IgG and HRP-IgG. The performance of Au/Pt NCs-IgG in a sandwich ELISA was compared with that of IgG tethered to the enzyme HRP of a conventional immunoassay. The calibration curve of the direct sandwich ELISA relying on Au/Pt NCs Anti-BSA IgG, prepared from IgG obtained from rabbit) is s ahown in Fig. 6A. In addition, the calibration curve obtained of a standard direct sandwich assay employing the same rabbit antibody tethered to HPR is shown in Fig 6B.

In both assays concentrations of Au/Pt NCs-IgG and IgG-HRP were optimised in order to get the best sensitivity. In order to optimise the concentration of detection antibody used in both ELISAs, capture antibody was immobilized on the surface of a well by adsorption overnight. After washing that various concentrations of BSA ranging from 0 to 200 ng/mL were added and incunbated. Next, upon washing, varying concentrations of detection IgG were injected into wells of the mictroplate. Fig S4 represents the initial rates of TMB oxidation obsereved in the immunoassays carried out in the presence and in the absence of BSA at different concentrations of o Au/Pt NCs-IgG and HRP-IgG.the signal to noise ratio for the system relying of Au/Pt NCs-IgG was 16.31 and that for the system relying on HRP-IgG was 3.54 (Fig. S5). After optimization of the experimental condition in terms of IgG concentrations the effect of various concentrations of the analyte on the read-out signals was studied.

In Fig. 6C and Fig. 6D the calibration curves for both systems are shown. The limit of detection (LOD) was calculated as three times of standard deviation of negative control divided by the slope of the regression line. A LOD of 0.93 ng/mL was achieved for the system using Au/Pt NCs-IgG. This value is 56 times better than that of the system using IgG-HRP, which demonstrated LOD of 52.03 ng/mL. Such a difference between LODs shown by two immunoassays can be explained by lower nonspecific adsorption of Au/Pt NCs IgG on the surface of a plastic microplate. Labeling of IgG with HRP by the crosslinking reaction leads to formation of byproducts prone to nonspecific absorption on a solid surface and consequently to an increase in the background signal.

Evaluation of the universality of the synthetic method for catalytic Au/Pt NCs-IgG and its application to various immunoassays. In order to evaluate universality and robustness of the new route to antibodies with peroxidase activity the synthesis of bimetallic NCs was carried out with two additional IgGs acting as scaffolds for the synthesis of NCs: Anti-Prostate specific antigen IgG (Anti-PSA IgG) and an Anti-Mouse IgG. The synthesis of the Au/Pt NCs Anti-PSA IgG and Au/Pt NCs Anti-Mouse IgG was performed as described in the experimental section with little changes. The concentration of IgG was changed to 0.5 mg/mL. The prepared Au/Pt NCs Anti-PSA IgG and Au/Pt NCs Anti-Mouse IgG exhibited peroxidase-like activity with the chromogenic substrate TMB in the presence of H_2O_2. Their catalytic properties were used in a direct ELISA to relate concentrations of PSA and an Anti-vinculin IgG from mouse respectively, with the reaction rate of TMB oxidation.

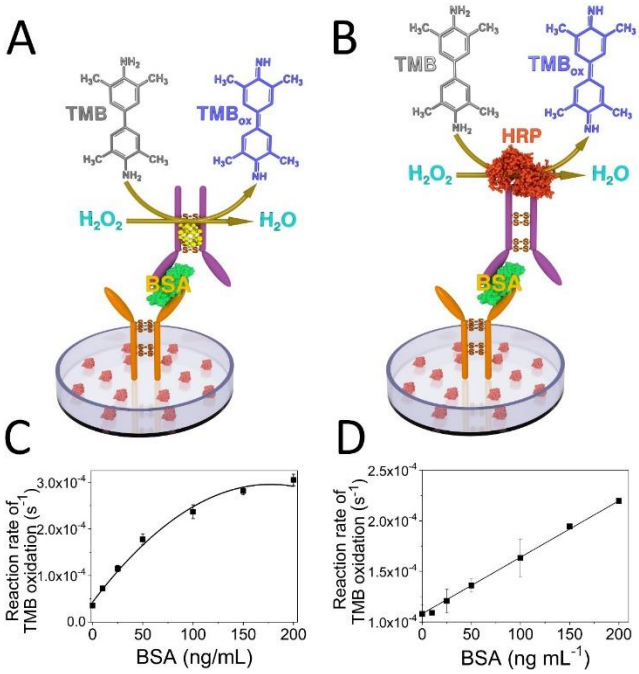

Figure 6. Schematic representation of direct sandwich ELISA for BSA quantification using the catalytic properties of Au/Pt NCs (A) or HRP-labelled (B) anti-BSA IgG. Calibration plot of BSA obtained in the sandwich ELISA for BSA based on Au/Pt NCs (C) and HRP-labelled (D) Anti-BSA IgG. Five replicates were employed for each BSA concentration.

To perform these immunoassays, first the surface of a MaxiSorp microplate was covered with different concentrations of PSA or Anti-vinculin IgG from mouse and incubated (overnight, 4 °C). Then, casein (100 µL, 20.5 mg/mL) was added as a blocking agent and incubated (1 h, RT). After, Au/Pt NCs Anti-PSA IgG (100 µL, 16 µg/mL) or Au/Pt NCs Anti-Mouse IgG (100 µL, 8 µg/mL) were added and incubated (1h, RT). Finally, the antigen concentration was related with the catalytic activity of the modified antibodies with 100 µL of TMB (200 µM) and H_2O_2 (250 mM). After each step the wells were washed three times with PBST (100 µL). In Fig. S6 the calibration curves for the direct ELISA for PSA and Anti-vinculin IgG from mouse are shown. The reaction rate of TMB oxidation increases with enhancing PSA and Anti-vinculin IgG from mouse concentrations. Thus, Au/Pt NCs Anti-PSA IgG and Au/Pt NCs Anti-Mouse IgG synthesized according to the present method retain their affinity to target analytes. Therefore, immunoassays for the quantification of PSA and Anti-vinculin IgG can be built using catalytic activity of Au/Pt clusters-

CONCLUSION

The experimental conditions for metallization of Au/Pt bimetallic nanoclusters inside of different antibodies were studied and optimized. These modified antibodies with high catalytic activity remain intact during the modification. Thus, IgGs still maintain affinity to their target analytes and Protein G. The Au/Pt NCs-IgG exhibit peroxidase-like activity and catalyze oxidation of the chromogenic substrate TMB in the presence of H_2O_2. The reaction catalyzed by the produced Au/Pt NCs IgG obeys the Michaelis-Menten law for enzymatic reactions. The increase in the substrate concentration results in the increase of the catalytic process rate. Synthesized Au/Pt-NCs IgG demonstrate quite high catalytic activity towards oxidation of TMB in the presence of hydrogen peroxide and lower nonspecific adsorption on solid surface in comparison with IgG tethered to HRP. The synthetic route to Au/Pt NCs IgG is robust and can be applied to the synthesis of different antibodies with catalytic activity. By using Au/Pt NCs-IgG instead of IgG-HRP the LOD for BSA was improved by 56 times.

ASSOCIATED CONTENT

Supporting Information. Synthesis optimization; comparison experiments between Au/NCs-IgG and HRP-IgG; catalytic activity of Au/Pt NCs anti-BSA IgG; electrophoretic analysis; TMB oxidation rate in the direct sandwich ELISA; ratio of read-out signals; and calibration curves obtained for detection of PSA and anti-vinculin IgG This material is available free of charge via the Internet at http://pubs.acs.org."

AUTHOR INFORMATION

Corresponding Author

* Valeri Pavlov . email: vpavlov@cicbiomagune.es

Author Contributions

The manuscript was written through contributions of all authors. All authors approved the final version of the manuscript.

Funding Sources

Ministry of Science, Innovation and Universities, Project BIO2017-88030-R and Maria de Maeztu Units of Excellence Programme – Grant No. MDM-2017-0720.

ACKNOWLEDGMENT

The authors gratefully acknowledge support from the Spanish Ministry of Science, Innovation and Universities (Project BIO2017-88030-R). We thank Dr. Di Silvio and Marco Möller for support with XPS and STEM measurements. Also we are grateful for EDX measurements with Dr. Sara Bals and her team from the University of Antwerp. This work was performed under the Maria de Maeztu Units of Excellence Programme – Grant No. MDM-2017-0720, Ministry of Science, Innovation and Universities

REFERENCES

(1) Hempen, C.; Karst, U. Labeling Strategies for Bioassays. *Anal. Bioanal. Chem.* **2006**, *384*, 572–583.

(2) Sakamoto, S.; Sakoda, J.; Morinaga, O.; Waraporn, P.; Tsuchihashi, R.; Morimoto, S.; Kinjo, J.; Tanaka, H. Development of an Enzyme Linked Immunosorbent Assay for Direct Determination of Anticancer Drug Vitamin K3 in Serum. *J. Heal. Sci.* **2008**, *54* (4), 508–511.

(3) Sakamoto, S.; Putalun, W.; Tsuchihashi, R.; Morimoto, S.; Kinjo, J.; Tanaka, H. Development of an Enzyme-Linked Immunosorbent Assay (ELISA) Using Highly-Specific Monoclonal Antibodies against Plumbagin. *Anal. Chim. Acta* **2007**, *607*, 100–105.

(4) Phrompittayarat, W.; Putalun, W.; Tanaka, H.; Wittaya-Areekul, S.; Jetiyanon, K.; Ingkaninan, K. An Enzyme-Linked Immunosorbant Assay Using Polyclonal Antibodies against Bacopaside I. *Anal. Chim. Acta* **2007**, *584*, 1–6.

(5) Thacker, J. D.; Casale, E. S.; Tucker, C. M. Immunoassays (ELISA) for Rapid , Quantitative Analysis in the Food-Processing Industry. *J. Agric. Food Chem.* **1996**, *44*, 2680–2685.

(6) Feng, J.; Huang, P.; Wu, F. Gold–platinum Bimetallic Nanoclusters with Enhanced Peroxidase-like Activity and Their Integrated Agarose Hydrogel-Based Sensing Platform for the Colorimetric Analysis of Glucose Levels in Serum. **2017**, *142*, 4106–4115.

(7) Avrameas, S. Coupling of Enzymes to Proteins with Glutaraldehyde. Use of the Conjugates for the Detection of Antigens and Antibodies. *Immunochemistry* **1969**, *6*, 43–52.

(8) Nakane, P. K.; Kawaoi, A. Peroxidase-Labeled Antibody a New Method of Conjugation. *J. Histochem. Cytochem.* **1974**, *22*, 1084–1091.

(9) Kato, K., Hamaguchi, Y., Fukui, H. and Ishikawa, E. Enzyme-Liked Immunoassay. A Simple Method for the Synthesis of the Rabbit Antibody-B-D-Galactosidase Complex and Its General Applicability. *J. Biochem.* **1975**, *78*, 423–425.

(10) Ishikawa, E. Enzyme-Labeling of Antibodies. In *Laboratory Techniques in Biochemistry and Molecular Biology*; 1999; pp 223–248.

(11) Guesdon, J. L.; Ternynck, T.; Avrameas, S. The Use of Avidin-Biotin Interaction in Immunoenzymatic Techniques. *J. Histochem. Cytochem.* **1979**, *27*, 1131–1139.

(12) Hui, W. and Erkang, W. Nanomaterials with Enzyme-like Characteristics (Nanozymes): Next-Generation Artificial Enzymes. *Chem. Soc. Rev.* **2013**, *42 (14)*, 6060–6093.

(13) Yang, H., Xiao,J., Su, L., Feng, T., Lv, Q. and Zhang, X. Oxidase-Mimic Activity of the Nitrogen-Doped Fe3C@C Composites. *Chem. Comm.* **2017**, *53*, 3882–3885.

(14) Jianshuai. M., Yan, W., Zhao, M. and Zhang, L. Intrinsic Peroxidase-like Activity and Catalase-like Activity of Co3O4 Nanoparticles W. *Chem. Commun* **2012**, *48*, 2540–2542.

(15) Asati, A.; Kaittanis, C.; Santra, S.; Perez, J. M. PH-Tunable Oxidase-Like Activity of Cerium Oxide Nanoparticles Achieving Sensitive Fluorigenic Detection of Cancer Biomarkers At. *Anal. Chem.* **2011**, *83*, 2547–2553.

(16) Zheng, A.-X.; Cong, Z.-X.; Wang, J.-R.; Li, J.; Yang, H.-H.; Chen, G.-N. Highly-Efficient Peroxidase-like Catalytic Activity of Graphene Dots for Biosensing. *Biosens. Bioelectron.* **2013**, *49*, 519–524.

(17) Tian, J.; Liu, Q.; Asiri, A. M.; Qusti, A. H.; Sun, Abdulrahman O. Al-Xuping, Y. Ultrathin Graphitic Carbon Nitride Nanosheets: A Novel Peroxidase Mimetic, Fe Doping-Mediated Catalytic Performance Enhancement and Application to Rapid, Highly Sensitive Optical Detection. *Nanoscale* **2013**, *5* (11604–11609), 11604–11609.

(18) Zheng, X.; Liu, Q.; Jing, C.; Li, Y.; Li, D.; Luo, W.; Wen, Y.; He, Y.; Huang, Q.; Long, Y.; et al. Catalytic Gold Nanoparticles for Nanoplasmonic Detection of DNA. *Angew. Chem.* **2011**, *50*, 11994–11998.

(19) Fan, J.; Yin, J.; Ning, B.; Wu, X.; Hu, Y.; Ferrari, M.; Anderson, G. J.; Wei, J.; Zhao, Y.; Nie, G. Direct Evidence for Catalase and Peroxidase Activities of Ferritin e Platinum Nanoparticles. *Biomat.* **2011**, *32*, 1611–1618.

(20) Stobiecka, M. Novel Plasmonic Fi Eld-Enhanced Nanoassay for Trace Detection of Proteins. *Biosens. Bioelectron.* **2014**, *55*, 379–385.

(21) Zheng, C., Zheng, A. X., Liu, B., Zhang, X. L.; He, Y., Li, J., Yang, H. H. and Chen, G. One-Pot Synthesized DNA-Templated Ag/Pt Bimetallic Nanoclusters as Peroxidase Mimics for Colorimetric Detection of Thrombin. *Chem. Commun.* **2014**, *50* (86), 13103–13106.

(22) Chen, L.-Y.; Wang, C.-W.; Yuan, Z.; Chang, H.-T. Fluorescent Gold Nanoclusters: Recent Advances in Sensing and Imaging. *Anal. Chem.* **2015**, *87* (1), 216–229.

(23) Le Guével, X. Recent Advances on the Synthesis of Metal Quantum Nanoclusters and Their Application for Bioimaging. *IEEE J. Sel. Top. Quantum Electron.* **2014**, *20* (3).

(24) Guo, S.; Wang, E. Noble Metal Nanomaterials : Controllable Synthesis and Application in Fuel Cells and Analytical Sensors. *Nano Today* **2011**, 240–264.

(25) Xie, J.; Zheng, Y.; Ying, J. Y. Protein-Directed Synthesis of Highly Fluorescent Gold Nanoclusters. *J. Am. Chem. Soc.* **2009**, *131* (3), 888–889.

(26) Das, T.; Ghosh, P.; Shanavas, M. S.; Maity, A.; Monda, S.; Purkayastha, P. Protein-Templated Gold Nanoclusters: Size Dependent Inversion of Fluorescence Emission in the Presence of Molecular Oxygen. *Nanoscale* **2012**, *4*, 6018–6024.

(27) Han, S.-Q.; Liu, J. L.; Gan, Z.-G.; Liang, J. G.; Zhao, S. M. Application of Luminescent BSA-Capped CdS Quantum Dots as a Fluorescence Probe for the Detection of Cu 2+. *J. Chinese Chem. Soc.* **2015**, *55*, 1069–1073.

(28) Ghosh, R.; Sahoo, A. K.; Ghosh, S. S.; Paul, A.; Chattopadhyay, A. Blue-Emitting Copper Nanoclusters Synthesized in the Presence of Lysozyme as Candidates for Cell Labeling. *ACS Appl. Mater. Interfaces* **2014**, *6*, 3822–3828.

(29) Zhou, T.; Huang, Y.; Cai, Z.; Luo, F.; Yang, C. J.; Chen, Y. Facile Synthesis of Red-Emitting Lysozyme-Stabilized Ag Nanoclusters. *Nanoscale* **2012**, *4* (17), 5312.

(30) Xia, X.; Long, Y.; Wang, J. Glucose Oxidase-Functionalized Fluorescent Gold Nanoclusters as Probes for Glucose. *Anal. Chim. Acta* **2013**, *772*, 81–86.

(31) Wen, F.; Dong, Y.; Feng, L.; Wang, S.; Zhang, S.; Zhang, X. Horseradish Peroxidase Functionalized Fluorescent Gold Nanoclusters for Hydrogen Peroxide Sensing Characterization. *Anal. Chem.* **2011**, *83*, 1193–1196.

(32) Ding, W.; Guan, L.; Han, J.; Mangala, R.; Luo, Z. Fluorescence Chemosensing of Water-Soluble Ag14nanoclusters for Lysozyme and Hg2+ions. *Sensors Actuators B* **2017**, *250*, 364–371.

(33) Schultz, D., Gardner, K., Oemrawsingh, S.R., Markeševič, N., Olsson, K., Debord, M., Bouwmeester, D. and Gwinn, E. Evidence for Rod-Shaped DNA-Stabilized Silver Nanocluster Emitters. *Adv. Mater.* **2013**, *25* (20), 2797–2803.

(34) Signor, L.; Erba, E. B. Matrix-Assisted Laser Desorption / Ionization Time of Flight (MALDI-TOF) Mass Spectrometric Analysis of Intact Proteins Larger than 100 KDa. *J. Vis. Exp.* **2013**, *79*, e50635.

(35) Davis, D. J.; Kyriakou, G.; Lambert, R. M. Uptake of n -Hexane , 1-Butene , and Toluene by Au / Pt Bimetallic Surfaces : A Tool for Selective Sensing of Hydrocarbons under High-Vacuum Conditions. *J. Phys. Chem B* **2006**, *110*, 11958–11961.

(36) Zeng, J.; Yang, J.; Lee, J. Y.; Zhou, W. Preparation of Carbon-Supported Core - Shell Au - Pt Nanoparticles for Methanol Oxidation Reaction : The Promotional Effect of the Au Core. *J. Phys. Chem B* **2006**, 24606–24611.

(37) Casaletto, M. P.; Longo, A.; Martorana, A.; Prestianni, A.; Venezia, A. M. XPS Study of Supported Gold Catalysts: The Role of Au0 and Au+d Species as Active Sites. *Surf. Interface Anal.* **2006**, *38*, 215–218.

(38) Lin, Y.; Chen, P.; Yuan, Z.; Ma, J.; Chang, H. The Isomeric Effect of Mercaptobenzoic Acids on the Preparation and Fluorescence Properties of Copper Nanoclusters. *Chem. Commun.* **2015**, *51*, 11983–11986.

(39) Wang, C.; Ling, L.; Yao, Y.; Song, Q. One-Step Synthesis of Fluorescent Smart Thermo- Responsive Copper Clusters : A Potential Nanothermometer in Living Cells. *Nano Res.* **2015**, *8*, 1975–1986.

(40) Jia, X.; Li, J.; Wang, E. Cu Nanoclusters with Aggregation Induced Emission Enhancement. *Small* **2013**, *9*, 3873–3879.

(41) Jiang, X.; Sun, C.; Guo, Y.; Nie, G.; Xu, L. Peroxidase-like Activity of Apoferritin Paired Gold Clusters for Glucose Detection. *Biosens. Bioelectron.* **2015**, *64*, 165–170.

(42) Wang, X.; Wu, Q.; Shan, Z.; Huang, Q. BSA-Stabilized Au Clusters as Peroxidase Mimetics for Use in Xanthine Detection. *Biosens. Bioelectron.* **2011**, *26*, 3614–3619.

(43) Gao, L.; Zhuang, J. I. E.; Nie, L.; Zhang, J.; Zhang, Y. U.; Gu, N.; Wang, T.; Feng, J.; Yang, D.; Perrett, S.; et al. Intrinsic Peroxidase-like Activity of Ferromagnetic Nanoparticles. **2007**, 577–583.

(44) Xian-ming, Q.; Liu, Z.; Cai, S.; Zhao, Y.; Wu, D. Electrochemical Aptasensor for the Detection of Vascular Endothelial Growth Factor (VEGF) Based on DNA-Templated Ag / Pt Bimetallic Nanoclusters. *Chin. Chem. Lett.* **2016**, No. 3677, 1–7.

(45) Joshi, V.; Shivach, T.; Yadav, N.; Rathore, A. S. Circular Dichroism Spectroscopy as a Tool for Monitoring Aggregation in Monoclonal Antibody Therapeutics. *Anal. Chem.* **2014**, *86* (23), 11606–11613.

(46) Vermeer, A. W. P.; Bremer, M. G. E. G.; Norde, W. Structural Changes of IgG Induced by Heat Treatment and by Adsorption onto a Hydrophobic Teflon Surface Studied by Circular Dichroism Spectroscopy. *Biochim. Biophys. Acta* **1998**, *1425*, 1–12.

(47) Daëron, M. Fc Receptor Biology. *Annu. Rev. Immunol.* **1997**, *15*, 203–234.

(48) Bagçi, H.; Kohen, F.; Kusçuoglu, U.; Bayer, E. A.; Wilchek, M. Monoclonal Anti-Biotin Antibodies Simulate Avidin m the Recognition of Biotin. *FEBS Lett.* **1993**, *322* (1), 47–50.

(49) Tan, Y. H.; Liu, M.; Nolting, B.; Go, J. G.; Gervay-Hague, J.; Liu, G. Y. A Nanoengineering Approach for Investigation and Regulation of Protein Immobilization. *ACS Nano* **2008**, *2* (11), 2374–2384.

SYNOPSIS TOC